Permeability, Form Drag Coefficient and Heat Transfer Coefficient of Porous Copper

Jan Mary Baloyo and Yuyuan Zhao*

School of Engineering, University of Liverpool, Liverpool L69 3GH, UK.

Corresponding author:

Professor Y. Y. Zhao
School of Engineering
University of Liverpool
Liverpool L69 3GH, UK.
Tel: 0044 151 7944697
Email: yyzhao@liverpool.ac.uk

Abstract

The water permeability, form drag coefficient and heat transfer coefficient of porous copper samples manufactured by the Lost Carbonate Sintering process were measured and analysed. The permeability increased and the form drag coefficient decreased with increasing porosity and decreasing pore size. There existed an empirical relationship between the form drag coefficient and the permeability. The highest heat transfer coefficient was observed at an optimum porosity of 60%, where heat removal by conduction and convection was balanced. Larger pore sizes led to higher heat transfer coefficients due to increased tortuosity and enhanced heat transfer by convection. The best overall heat transfer performance with a combination of high Nusselt number and low friction factor was achieved at the porosity of 65%.

Introduction

Metal foams have attracted much attention in both academia and industry in the past three decades due to their unique mechanical, chemical, electrical and thermal properties, e.g., high specific stiffness, high surface area, electromagnetic shielding effect and good heat dissipation capacity [1-4]. Fluid flow in open-cell metal foams is one of the areas of interest to the thermo-fluids and materials manufacturing research communities because of their importance in numerous applications. For example, metal foams have high internal surface area and high permeability for fluids, which make them ideal candidate materials for thermal management applications, e.g., as heat exchangers or cooling systems for electronic devices [5-11]. A typical metal foam cooling system consists of a liquid or gas coolant flowing through the internal pores or channels of the porous medium. Heat is transferred from the heated device to the metal foam by conduction and carried away by the flowing coolant by convection. The fluid flow of the coolant inside the porous structure often dictates the efficacy of the heat transfer and the pressure drop across the foam directly determines the power required for pumping the fluid.

An overview of the governing equations of flow in porous media was presented by Dukhan [12]. The relationship between pressure drop and flow velocity for one-dimensional flow in a porous medium is often described by the Darcy equation [6]:

$$\frac{\Delta P}{L} = \frac{\mu}{K} v_D \tag{1}$$

where ΔP is the pressure drop (Pa), L is the length of the porous medium (m), μ is the dynamic viscosity of the fluid (Pa·s), K is the permeability (m^2), and v_D is the Darcian velocity ($m \cdot s^{-1}$), which is obtained by dividing the volumetric fluid flow rate by the cross-sectional area of the porous medium. However, Darcy equation is only applicable for creeping flow where only viscous drag is present, with the permeability based Reynolds number in the order of unity or less [12].

For sufficiently high flow velocities, form drag becomes important and Darcy equation has to be modified. In these cases, the pressure drop behaviour is described by the Forchheimer equation [6]:

$$\frac{\Delta P}{L} = \frac{\mu}{K} v_D + \rho C v_D^2 \quad (2)$$

where ρ is the density of the fluid (kg·m^{-3}) and C is a form drag coefficient (m^{-1}).

The most widely cited correlation between pressure drop and the structural parameters of porous media is Ergun's equation [6], which was developed for packed beds of solid spherical particles:

$$\frac{\Delta P}{L} = \frac{150(1-\varepsilon)^2 \mu}{\varepsilon^3 d^2} v_D + \frac{1.75(1-\varepsilon)\rho}{\varepsilon^3 d} v_D^2 \quad (3)$$

where ε is porosity and d is particle diameter. Ergun's equation is only valid for granular media with porosities ranging from 0.38 to 0.47 and not for foams or fibrous media [13]. Most empirical correlations proposed for other porous media were extensions of Ergun's equation by adopting a characteristic feature (e.g., ligament diameter) as an equivalent particle diameter and by modifying the values of the constants (including the exponents of porosity and particle diameter terms) to fit the experimental data for the porous media in investigation. In most cases, the permeability and form drag coefficient terms were correlated to porosity and pore size, or equivalent particle diameter [14,15]. Occasionally, other parameters (e.g., tortuosity [16]) were included. Generally, no correlation applies to all porous media and each type of porous materials has to be considered separately.

A considerable amount of research has been carried out recently on the heat transfer behaviour of metal foams. Ejlali *et al*. [5] numerically investigated the applicability of high-porosity metal foams as air-cooled heat exchangers for geothermal power plants and found that

metal foam heat exchangers are superior compared to conventional finned surfaces with no excessive trade-offs (material weight and/or pressure drop). Boomsma *et al*. [17] demonstrated experimentally that compressed open-cell aluminium metal foam heat exchangers generated thermal resistances 2-3 times lower than the best commercially available heat exchanger tested under a similar pumping power. Similarly, Mao *et al*. [18] demonstrated that the heat transfer capability of metal foam heat exchangers can supersede conventional compact heat exchangers given optimal scenarios (i.e. optimal porosity and foam thickness). Hutter *et al*. [19] reviewed the factors that greatly influence the heat transfer performance of porous metal-coolant heat exchangers, and reported that the coolant properties (e.g. heat capacity or thermal conductivity) have a significant influence on the convective heat transfer of the metal-foam system. Zhao [7] reviewed comprehensively the research progress on the heat transfer in metal foams for thermal management applications. These reports showed that the fluid flow and heat transfer are invariably interlinked and the choice of the foam material also influences the heat transfer performance significantly. The foam structure considerably affects the heat transfer performance, with porosity, pore size and surface area having the greatest weightings on the effective thermal conductivity, convective heat transfer and fluid flow properties.

However, very limited amount of research has been conducted on the fluid and heat transfer behaviour of metal foams made by the space-holder methods, where the pores are created by using a sacrificial powder (space holder), such as NaCl [20], K_2CO_3 [21] or ammonium bicarbonate [22]. The pores are negative replicas of the sacrificial powder particles, so that the porosity and pore size can be independently varied. The metal foams produced by the space holder methods have distinctive porous structures (internal architecture) which are very different from those of the packed beds and metal foams produced by the other methods. Firstly, their porosities are normally

in the range of 50 – 85%, while packed beds and granular media have much lower porosities (30-60%) and the aluminium foams studied so far usually have higher porosities (80 – 95%). Secondly, the voids in the metal foams produced by space holder methods are individual spherical pores randomly distributed in a metal matrix and interconnected through windows much smaller than the pores. In packed beds, the voids are the interstices between solid spherical particles, forming irregular shaped narrow channels. In high porosity aluminium foams, the voids are a large open space partitioned with a network of narrow solid struts. Thirdly, they have rough internal surfaces formed by bonding of small metal particles, while the packed beds or aluminium foams have relatively smooth surfaces formed by sand particles or cast aluminium struts. Preliminary studies [23, 24] showed that the flow resistance experienced in the foams produced by the space holder methods and the heat transfer behaviour are very different from those in packed beds or other foams manufactured by a different process. However, the fluid flow and thermal behaviours, especially the relationship between the permeability and form drag coefficient and the interactions between flow resistance and heat transfer, are not well understood.

In this paper, we study the fluid flow and heat transfer performance in copper foams produced by the Lost Carbonate Sintering (LCS) process, a typical space holder method which can be used to generate porous structures representative of all metal foams produced by the space-holder family. The structural effects (porosity and pore size) on the permeability, form drag coefficient and heat transfer coefficient are studied. Correlations between permeability and form drag coefficient and between flow resistance and heat transfer coefficient are investigated.

Experimental details

Nineteen porous copper samples with different porosities (50-80%) and pore sizes (250-1500 μm) were fabricated using the LCS process [20]. The Cu powder (base metal) was supplied by Ecka Granules UK Ltd. and had a particle size range of 75 μm to 150 μm and a purity of 99.9%. The food grade K_2CO_3 powder (space holder) was manufactured by E&E Ltd. and had a particle size range of 250 μm to 1500 μm and >98% purity. The K_2CO_3 powder was sieved and categorized to four different size ranges: 250-425 μm, 425-710 μm, 710-1000 μm and 1000-1500 μm, resulting in copper foams with four pore size ranges. The porosity of the samples was measured using the Archimedes method.

Fig. 1 shows the representative microstructure of the as-produced LCS porous copper. Small voids (inter-particle pores) between the copper particles allow the interconnection between the pores created by the K_2CO_3 particles, enhancing the sample's permeability to fluids.

The pressure drops and heat transfer coefficients in the LCS porous copper samples were measured using a purpose-built apparatus with a polytetrafluoroethylene (PTFE) chamber as described in [6] and shown schematically in Fig. 2, using water as the working fluid. For heat transfer tests, seven 100W heat cartridges were imbedded in the oxygen-free copper heat block to supply the heat flow. The heat cartridges were controlled by a variac (voltage range of 10-240 V). Attached to the heat block is another oxygen-free copper block with the same cross section as the porous copper sample (30 mm × 20 mm), and was pressed tightly against the porous copper sample to achieve good thermal contact. The temperatures at the top (T_t) and bottom (T_b) spots of the lower copper block were measured after a steady state condition was reached using T-type thermocouples

(±0.1% accuracy). The heat flux through the lower copper block, *J*, is equivalent to the heat flux to the sample and was calculated by:

$$J = k_{Cu} \frac{T_t - T_b}{s} \quad (4)$$

where *s* is the distance between the spots for measuring T_t and T_b (30 mm), and k_{Cu} is the thermal conductivity of the oxygen free copper block. The input voltage was varied between 60 V to 150 V to produce different heat fluxes.

During the experiment, the water coolant flowed through 1) a filter, 2) a flow meter (Omega FL50001A, ±5% accuracy), 3) a pressure transducer (Omega PXL 219-004GI, ±0.25% accuracy, 0-4 bar pressure range) to measure the inlet pressure, P_{in}, 4) a thermometer (PT 100, ±0.1°C accuracy) to measure the inlet fluid temperature, T_{in}, 5) the porous copper in the sealed chamber, and 6) another pressure transducer (Omega PXM219-001G, ±0.25%, 0–1 bar pressure range) to measure the fluid's outlet pressure, P_{out}. All samples were 30 mm long, 20 mm wide and 5 mm high, which tightly fit into the channel. The overall heat transfer coefficient (*U*) of the cooling system, which is made of the porous copper sample and the water coolant, was determined by:

$$U = \frac{J}{T_b - T_{in}} \quad (5)$$

The pressure drop across the copper foam sample was measured at room temperature at different flow rates (up to 2 L/min, *Re* = 5 – 140) and was normalised against the respective length of the sample. All the data used are the averages of the values of three experimental measurements. The physical properties of copper and water used to calculate permeability, form drag coefficient, overall heat transfer coefficient and Nusselt number are listed in Table 1.

Uncertainty analysis

Pressure drop

The pressure drop, ΔP, is the difference between inlet water pressure P_{in} and outlet water pressure P_{out},

$$\Delta P = P_{in} - P_{out} \tag{6}$$

where P_{in} and P_{out} were measured by two precision pressure gauges with an accuracy of 0.01 bar (ω_P). The uncertainty of pressure drop, $\omega_{\Delta P}$, can be calculated by propagation of uncertainty as follows:

$$\omega_{\Delta P} = \sqrt{(\frac{\partial \Delta P}{\partial P_{in}}\omega_P)^2 + (\frac{\partial \Delta P}{\partial P_{out}}\omega_P)^2} \tag{7}$$

which gives $\omega_{\Delta P}$ = 0.014 bar.

The uncertainty of pressure drop per unit length ($\Delta P/L$), $\omega_{\Delta P/L}$, can be calculated by

$$\omega_{\Delta P/L} = \sqrt{(\frac{\partial \Delta P/L}{\partial \Delta P}\omega_{\Delta P})^2 + (\frac{\partial \Delta P/L}{\partial L}\omega_L)^2} \tag{8}$$

The sample length (L) is 0.03 m and its accuracy is 0.0005 m (ω_L). The typical pressure drop is 1.235 bar. These give the uncertainty of pressure drop per unit length, $\omega_{\Delta P/L}$ = 0.007 bar/m.

Heat transfer coefficient

The overall heat transfer coefficient, U, was calculated using:

$$U = \frac{k_{Cu}\,(T_t - T_b)}{s\,(T_b - T_{in})} \tag{9}$$

where k_{Cu} is the thermal conductivity of the Cu heating block (390 W/mK), T_t and T_b are the temperatures of the block at the top and bottom (Fig. 2), which were measured by T-type thermocouples with an accuracy (ω_T) of 0.5˚C, and s is the distance between the two temperature measurement spots (ω_s= 0.0005 m). According to the propagation of uncertainty, the uncertainty of heat transfer coefficient (ω_U) can be calculated by:

$$\omega_U = \sqrt{(\frac{\partial U}{\partial s}\omega_s)^2 + (\frac{\partial U}{\partial T_t}\omega_T)^2 + (\frac{\partial U}{\partial T_b}\omega_T)^2 + (\frac{\partial U}{\partial T_{in}}\omega_T)^2} \quad (10)$$

which gives an uncertainty of ω_U = 0.324 kW/(m^2·K).

Results and discussion

Pressure drop

The length-normalised pressure drops for the LCS porous copper samples at different water flow rates (up to 2 L/min) are shown in Fig. 3. The pressure drop for all the samples increased with increasing Darcian velocity in a quadratic fashion. All quadratic curves fitted well with the Forchheimer's equation (Eq. 2), with a determination coefficient R^2>99%, from which the permeability *K* and form drag coefficient *C* values were obtained.

It is shown that the porosity of the LCS porous copper samples significantly affects the pressure drop. For each pore size category, the sample with the lowest porosity gave the highest pressure drop at any given water flow rate. For samples with different pore size ranges but a similar porosity, the samples with smaller pore sizes generated lower pressure drops than the samples with larger pores.

Effects of porosity and pore size on permeability

The relationships between permeability (*K*) and porosity of the LCS porous copper samples with different pore sizes are displayed in Fig. 4. The results fall on the same trendline as those reported by Xiao and Zhao [6] for LCS porous metals with a pore size range 425 – 710 μm. The porosity of the LCS porous copper consists of the large pores (primary porosity) created by the space-holder particles and the small inter-particle pores (secondary porosity) created through bonding of Cu particles (Fig. 1). Porosity has a significant effect on the permeability. In general, there is an exponential relationship between permeability and porosity, similar to that found in [25,

26]. Increasing porosity leads to lower fluid resistance since there is a lower fraction of solid matrix impeding fluid flow. Furthermore, the likelihood of the pores being connected to each other is higher in samples with higher porosity than found in the lower porosity samples. Consequentially, the pressure drop decreases and hence, the water permeability of the samples increases with increasing porosity.

The pore size also influences the water permeability, with higher permeability values recorded for samples with smaller pore sizes, as shown in Fig. 4. Several reports on porous media also showed that smaller pore sizes led to higher water permeability [27-29]. This is because pore size affects the number and tortuosity of flow channels of the porous media. Decreasing the pore size leads to an increase in pore density per unit volume, so that the pores become more connected and more channels for fluid flow are created. As a result, the resistance to water flow decreases, leading to lower pressure drops and higher permeability.

Diao *et al*. [30] measured the tortuosity of LCS porous Cu using a diffusion diaphragm cell. They showed that the tortuosity increased with pore size and decreased with porosity, and the relationship between tortuosity and porosity followed a correlation developed for porous materials with a porosity range from 0.5 to 1 [31]:

$$\tau = p(1-\varepsilon) + 1 \tag{11}$$

where τ is tortuosity, p is a fitting parameter and ε is porosity. They further showed that the fitting parameter p increased nearly linearly with pore size. The other correlations [32], e.g., developed for packed beds [33], randomly placed rectangles [34] and extremely high or low porosity media [35] are found to be less suitable for LCS porous metals.

Fig. 5 shows the relationship between the water permeability and tortuosity, where the tortuosity values are taken from [30] for the LCS porous Cu samples with the same pore sizes and

porosities. It is shown that permeability correlates strongly with tortuosity, with the former decreasing exponentially with the latter. For the same tortuosity, the samples with smaller pores have considerably higher permeability than those with larger pores.

It is worth noting that several studies on aluminium metal foams, e.g. [36, 37], found that permeability increased as the pore size increased. This contradiction is due to the very different pore structures between the LCS porous metal and the aluminium foams. The aluminium foams used in [36, 37] were manufactured by the investment casting method replicating a polymeric foam structure. These foams had an initial porosity greater than 90% and were compressed to achieve lower porosities. In these foams, a three-dimensional network of metal struts are surrounded by a far larger open space. Although a pore size was used in [36, 37] to define a space separated by sparsely connected metal struts, the open space cannot really be divided into meaningful pores as in LCS porous copper. The flow resistance in these high-porosity foams are generated from the metal struts and, in our opinion, cannot be attributed to pores.

Effects of porosity and pore size on form drag coefficient

The relationship between the form drag coefficient and the structural parameters of the LCS porous copper samples, porosity and pore size, is shown in Fig. 6. The form drag coefficients of several low porosity samples are not shown because accurate values could not be obtained from the limited data points for these samples. Fig. 6 shows that the form drag coefficient decreases with increasing porosity and decreasing pore size. These findings are consistent with those found in literature [14, 16, 27, 28, 38]. This is because a higher porosity means a lower fraction of solid impeding the fluid flow, resulting in a lower fluid resistance and thus a higher form drag coefficient. Samples with larger pores have more tortuous channels for fluid flow [30], resulting in a higher fluid resistance and thus a lower form drag coefficient.

Permeability and form drag coefficient are hydrodynamic properties describing how easy a fluid can flow through the porous medium and signifying the viscous and form drag behaviours of the porous medium, respectively. Both are dependent on the internal architecture of the porous medium, i.e., porosity, pore morphology, pore size, and the distribution and 'connectedness' of the pores and are often interdependent [39]. Avalos-Gauna and Zhao [40] created a 3D geometric model to simulate the LCS porous structure based on the face-centred-cubic arrangement of spheres linked by cylinders. They calculated the permeability and form drag coefficient for different combinations of pore parameters, including porosity and pore size, by numerical simulation using computational fluid dynamics software. They showed that the form drag coefficient is related to the permeability by:

$$C = C_f K^{-m} \tag{12}$$

where C_f is the drag force coefficient and m is an exponential term. Both C_f and m are constant for any given pore size, but C_f increases and m decreases with increasing pore size. Fig. 7 shows the log–log plot between form drag coefficient and permeability for the LCS porous Cu samples measured in the study. It shows that the form drag coefficient decays exponentially with permeability, with the C_f and m values of 3.21 and 0.76, respectively, fitting reasonably well with the data for all the pore size ranges. In other words, the effect of pore size on C_f and m seems to be insignificant.

Effects of porosity and pore size on heat transfer coefficient

Fig. 8 displays the variations in heat transfer coefficient with porosity. For comparison, the heat transfer coefficients of the empty chamber with water flow only (100% porosity) were also measured and included, as well as those reported in [6]. For any sample, the heat transfer

coefficient increased with increasing water flow rate, because heat removal by convection occurs more rapidly at higher water flow rates. Additionally, at a higher water flow rate, the flow may become more turbulent, increasing flow mixing and promoting greater flow access to inter-particle pores within the porous structure. Consequently, a larger copper surface comes into contact with the coolant, enhancing the heat transfer between the two media.

Fig. 8 shows that the sample's porosity has a strong influence on the heat transfer coefficient, showing the same trend as that reported in [6]. For samples with low porosities (~46% and ~54%), the heat transfer coefficients were very small for all the water flow rates. Increasing the porosity to approximately 60% led to a sharp rise in the heat transfer coefficient. Increasing the sample's porosity further led to the gradual decline in the heat transfer coefficient. This suggests that there exists an optimum porosity offering the maximum heat transfer coefficient for LCS homogeneous samples, which is approximately 60% for the pore size range of 425-710 μm.

Heat removal within the LCS porous copper - water cooling system occurs through thermal conduction and thermal convection. Heat from the heat source is transported to the LCS copper sample by conduction and is removed subsequently by the flowing water coolant through convection. The overall heat transfer performance of the LCS porous copper sample is therefore determined by the parameters affecting these processes, i.e., the sample's thermal conductivity and the sample's permeability to the coolant.

For samples with low porosity (< 60%), there is a high volume of copper present, resulting in high thermal conductivity [41]. However, a high volume of copper also means more resistance to fluid flow, as discussed in the previous section. Samples with low porosity have low internal passage for fluid flow and low fluid permeability, leading to poor heat removal by the water

coolant through convection. Even though low porosity samples have good thermal conductivity, the overall heat transfer performance is limited by the poor thermal convection within the structure.

On the other hand, the high porosity LCS Cu samples (> 60%) have a small volume of copper. This leads to high internal passage and high permeability for fluid, enhancing heat removal by thermal convection as a consequence. However, thermal conductivity within the high porosity samples is compromised since there is a smaller volume of copper present to conduct heat. As a consequence, the overall heat transfer performance is limited by the thermal conduction of the porous copper matrix.

At the optimum porosity of ~60%, heat removal by thermal conduction through the copper matrix and thermal convection from the matrix to the flowing coolant is balanced. Compared to an empty chamber (100% porosity), the heat transfer coefficient is approximately four times greater. This demonstrates that LCS porous copper can greatly improve the heat transfer performance and is suitable for thermal management applications.

The heat transfer coefficients of three samples of similar porosity but different pore sizes, at varying water flow rates, are displayed in Fig. 9. The heat transfer coefficient increases with increasing pore size at any given water flow rate. Samples with smaller pores have lower tortuosities [30]. As a consequence, the fluid flow passes through the sample more quickly and dwells in the sample for a shorter period of time, which may reduce heat transfer by convection. Samples with larger pores, on the other hand, have higher tortuosities [30] and can therefore improve the effectiveness of convectional heat transfer. In addition, inertial effects (form drag) are greater in samples with larger pores, as discussed in the previous section. This may induce a more turbulent flow, leading to greater mixing and greater access to smaller channels within the

structure. Heat removal by convection can therefore be enhanced, resulting in better heat transfer performance.

Friction factor and Nusselt number

Friction factor characterises dimensionless pressure drop and represents the effect of the system and operating parameters, including the internal surface condition and surface roughness. The friction factor (*f*) for the internal flow within the LCS porous structure can be expressed as:

$$f = \frac{\Delta P\ D}{L\ \rho v^2} \tag{13}$$

where *D* is the pore diameter and *v* is the fluid velocity within the pores, which is related to Darcian velocity by $v = v_D/\varepsilon$. The real fluid velocity, instead of Darcian velocity, is used here, because it is the former that generates the fluid friction with the pore walls.

Nusselt number is the ratio of convective to conductive heat transfer. The Nusselt number (*Nu*) for the LCS porous copper samples can be expressed as:

$$Nu = \frac{UD}{k_F} \tag{14}$$

where k_F is the thermal conductivity of water.

Fig. 10 displays the variations of Nusselt number and friction factor with sample porosity and Reynolds number for the samples with the same pore size of 425 – 710 μm. The Reynolds number was calculated by:

$$Re = \frac{\rho v D}{\mu} \tag{15}$$

Again, the real fluid velocity within the pores, instead of Darcian velocity, is used in defining the Reynolds number, because it is the former that dictates the flow regimes and the transition from one regime to another. With increasing Reynolds number, the Nusselt number increased while the friction factor decreased, agreeing with the results reported by various researchers [42-45].

There are three distinct regions in Fig. 10. The samples with low porosities of 45.8% and 54.2% have low Nusselt numbers and high friction factors spanning a wide range. The sample with a porosity of 59.2% has the highest Nusselt number among all samples for any given Reynolds number. Its friction factor, however, is also high and is in similar range as those of the 45.8% and 54.2% porosity samples. The samples with high porosities ranging from 63.8% to 77.0% have relatively high Nusselt numbers and very low friction factors. The overall heat transfer performance, i.e., a combination of high Nusselt number and low friction factor, is obtained at the porosity of 63.8% for the LCS porous copper.

Conclusions

1) The pressure drop for the LCS porous Cu samples increased with increasing Darcian velocity and fitted well with the Forchheimer's equation. The water permeability increased exponentially with increasing porosity and decreased slightly with increasing pore size. The relationship between the form drag coefficient C and the permeability K was well described by $C = 3.21K^{-0.76}$ for all samples.
2) The heat transfer coefficient increased with increasing water flow rate. A porosity of ~60% resulted in the highest heat transfer coefficient, because of balanced heat removal by conduction and convection. Lower or higher porosities led to lower heat transfer coefficient due to limited conduction or convection. Large pores resulted in higher heat transfer coefficients because of higher tortuosities and thus longer fluid dwell times in the samples.
3) The Nusselt number increased and the friction factor decreased with Reynolds number. Both the Nusselt number and the friction factor were sensitive to porosity. A porosity of ~65% resulted in the best overall heat transfer performance, a combination of high Nusselt number and low friction factor.

Acknowledgements

This work was supported by the Engineering and Physical Sciences Research Council (Grant No. EP/N006550/1); the Centre for Global Eco-Innovation of the University of Liverpool; and Versarien plc.

Nomenclature

C	form drag coefficient, m^{-1}
Cu	copper
D	pore diameter, m
d	particle diameter, m
f	friction factor
J	heat flux, W/m^2
K	permeability, m^2
k	thermal conductivity, W/(m·K)
K_2CO_3	potassium carbonate
L	length of the porous medium or flow length, m
LCS	Lost Carbonate Sintering
m	fitting constant
Nu	Nusselt number
P	pressure, Pa
p	fitting constant
PTFE	Polytetrafluoroethylene
Re	Reynolds number
s	distance between T_t and T_b, m
SEM	Scanning Electron Microscope
T	temperature, K
U	overall heat transfer coefficient, $W/(m^2 \cdot K)$
v	velocity, m/s

Greek Symbols

ε	porosity
μ	fluid dynamic viscosity, Pa·s
ρ	fluid density, kg/m^3
τ	tortuosity
ω	uncertainty

Subscripts

b	bottom region
Cu	copper
D	Darcian

F	fluid (water)
f	drag force
in	inlet
L	length
out	outlet
P	pressure
s	distance
T	temperature
t	top region
U	overall heat transfer coefficient
ΔP	pressure difference
$\Delta P/L$	length normalised pressure difference

References

[1] J. Banhart, M. Ashby, and N. Fleck, *Metal Foams and Porous Metal Structures*. Breman, Germany: MIT Publishing, 1999.

[2] L. Gibson and M. Ashby, *Cellular Solids*, Oxford, UK: Pergamon Press, 1998.

[3] J. Banhart, "Manufacture, characterisation and application of cellular metals and metal foams," *Prog. Mater. Sci.*, vol. 46, no. 6, pp. 559-632, 2001. DOI: 10.1016/S0079-6425(00)00002-5.

[4] S. Miwa, and S. T. Revankar, "Hydrodynamic characterization of nickel metal foam—effects of pore structure and permeability," *Heat Transfer Eng.*, vol. 33, no. 9, pp. 800-808, 2012. DOI: 10.1080/01457632.2012.646872.

[5] A. Ejlali, A. Ejlali, K. Hooman, and H. Gurgenci, "Application of high porosity metal foams as air-cooled heat exchangers to high heat load removal systems," *Int. Commun. in Heat and Mass Transfer*, vol. 36, no. 7, pp. 674-679, 2009. DOI: 10.1016/j.icheatmasstransfer.2009.03.001.

[6] Z. Xiao, and Y. Y. Zhao, "Heat transfer coefficient of porous copper with homogeneous and hybrid structures in active cooling," *J. Mater. Res.*, vol. 28, no. 17, pp. 2545-2553, 2013. DOI: 10.1557/jmr.2013.190.

[7] C. Y. Zhao, "Review on thermal transport in high porosity cellular metal foams with open cells," *Int. J. Heat Mass Tran.*, vol. 55, no.13-14, pp. 3618-3632, 2012. DOI: 10.1016/j.ijheatmasstransfer.2012.03.017.

[8] I. Ghosh, "How good is open-cell metal foam as heat transfer surface?," *J. Heat Transfer*, vol. 131, no. 10, pp. 101004-101012, 2009. DOI: 10.1115/1.3160537.

[9] S. E. Rad, H. Afshin, and B. Farhanieh, "Heat Transfer enhancement in shell-and-tube heat exchangers using porous media," *Heat Transfer Eng*., vol. 36, no. 3, pp. 262-277, 2015. DOI: 10.1080/01457632.2014.916155.

[10] T.-M. Jeng, and S.-C. Tzeng, "Forced convection of metallic foam heat sink under laminar slot jet confined by parallel wall," *Heat Transfer Eng*., vol. 28, no. 5, pp. 484-495, 2007. DOI: 10.1080/01457630601166127.

[11] Y. Wang, J. Wang, and P. Jia, "Performance of forced convection heat transfer in porous media based on gibson–ashby constitutive model," *Heat Transfer Eng*, vol. 32, no. 11-12, pp. 1093-1098, 2011. DOI: 10.1080/01457632.2011.556508.

[12] N. Dukhan, *Metal Foams: Fundamentals and Applications*, Lancaster, PA, USA: DEStech Publications, Inc., 2013.

[13] E. Haque, "Void fraction as a function of depth and pressure drops of packed beds of porous media formed by granular materials," *Trans. ASABE*, vol. 54, no. 6, pp. 2239-2243, 2011. DOI: 10.13031/2013.40636

[14] J. Geertsma, "Estimating the coefficient of inertial resistance in fluid flow through porous media," *SPE J.*, vol. 14, no. 5, pp. 445-450, 1974. DOI: 10.2118/4706-PA.

[15] L. Tadrist, M. Miscevic, O. Rahli, and F. Topin, "About the use of fibrous materials in compact heat exchangers," *Exp. Therm. Fluid Sci*., vol. 28, no. 2-3, pp. 193-199, 2004. DOI: 10.1016/S0894-1777(03)00039-6.

[16] X. Liu, F. Civan, and R. D. Evans, "Correlation of the non-Darcy flow coefficient," *J. Can. Petrol Technol*., vol. 34, no. 10, pp. 50-54, 1995. DOI: 10.2118/95-10-05.

[17] K. Boomsma, D. Poulikakos, and F. Zwick, "Metal foams as compact high performance heat exchangers," *Mech. Mater.*, vol. 35, no. 12, pp. 1161-1176, 2003. DOI: 10.1016/j.mechmat.2003.02.001

[18] S. L. Mao, N. Love, A. Leanos, and G. Rodriguez-Melo, "Correlation studies of hydrodynamics and heat transfer in metal foam heat exchangers," *Appl. Therm. Eng*, vol. 71, no. 1, pp. 104-118, 2014. DOI: 10.1016/j.applthermaleng.2014.06.035.

[19] C. Hutter, D. Buchi, V. Zuber, and P. R. von Rohr, "Heat transfer in metal foams and designed porous media," *Chem. Eng. Sci*., vol. 66, no. 17, pp. 3806-3814, 2011. DOI: 10.1016/j.ces.2011.05.005.

[20] Y. Y. Zhao, and D. X. Sun, "A novel sintering-dissolution process for manufacturing Al foams," *Scripta Mater*., vol. 44, no. 1, pp. 105-110, 2001. DOI: 10.1016/S1359-6462(00)00548-0.

[21] Y. Y. Zhao, T. Fung, L.P . Zhang, and F. L. Zhang, "Lost carbonate sintering process for manufacturing metal foams," *Scripta Mater*., vol. 52, no. 4, pp. 295-298, 2005. DOI: 10.1016/j.scriptamat.2004.10.012.

[22] A. Laptev, O. Vyal, M. Bram, H. Buchkremer, and D. Stöver, "Green strength of powder compacts provided for production of highly porous titanium parts," *Powder Metall*., vol. 48, no. 4, pp. 358-364, 2005. DOI: 1 0.1179/174329005X73838.

[23] P. Khayargoli, V. Loya, L. P. Lefebvre, and M. Medraj, "The impact of microstructure on the permeability of metal foams," in *Proc. the CSME 2004*, London, Canada, 1-4 June 2004, pp. 220-228.

[24] K. Diao, X. Lu, Z. Wu, and Y. Zhao, "Heat transfer performance of LCS porous copper with different structural characteristics," *Materials Science Forum*, vol. 933, pp. 380-387, October 2018. DOI: 10.4028/www.scientific.net/MSF.933.380.

[25] P. H. Nelson, "Permeability-porosity relationships in sedimentary rocks," *Log. Analyst*, vol. 35, no. 3, pp. 38-62, 1994.

[26] C. M. Bethke, "A numerical-model of compaction-driven groundwater-flow and heat-transfer and its application to the paleohydrology of intracratonic sedimentary basins," *J. Geophys. Res-Solid*, vol. 90, no. 8, pp. 6817-6828, 1985. DOI: 10.1029/JB090iB08p06817.

[27] H. Y. Zhang, et al., "Fluid flow and heat transfer in liquid cooled foam heat sinks for electronic packages," *IEEE T. Compon. Pack. T.*, vol. 28, no. 2, pp. 272-280, 2005. DOI: 10.1109/TCAPT.2005.848528.

[28] J. P. Bonnet, F. Topin, and L. Tadrist, “Flow laws in metal foams: compressibility and pore size effects,” *Transp. Porous Med.*, vol. 73, no. 2, pp. 233-254, 2008. DOI: 10.1007/s11242-007-9169-5.

[29] J. F. Despois, and A. Mortensen, “Permeability of open-pore microcellular materials,” *Acta Mater*., vol. 53, no. 5, pp. 1381-1388, 2005. DOI: 10.1016/j.actamat.2004.11.031.

[30] K. K. Diao, L. P. Zhang, and Y.Y . Zhao, “Measurement of tortuosity of porous copper using a diffusion diaphragm cell,” *Measurement*, vol. 110, pp. 335-338, November 2017. DOI: 10.1016/j.measurement.2017.07.014.

[31] A. Koponen, M. Kataja, and J. Timonen, “Tortuous flow in porous media,” *Phys. Rev. E. Stat. Phys. Plasmas. Fluids Relat. Interdiscip. Topics*, vol. 54, no. 1, pp. 406-410, 1996. DOI: 10.1103/PhysRevE.54.406.

[32] B. Ghanbarian, A.G. Hunt, R. Ewing and M. Sahimi, “Tortuosity in porous media: a critical review,” *Soil Sci. Soc. Am. J.*, vol. 77, pp. 1461–1477, September 2013. DOI:10.2136/sssaj2012.0435.

[33] P.-Y. Lanfrey, Z.V. Kuzeljevic, and M.P. Dudukovic, “Tortuosity model for fixed beds randomly packed with identical particles,” *Chem. Eng. Sci*., vol. 65, pp. 1891–1896, March 2010. DOI: 10.1016/j.ces.2009.11.011.

[34] A. Koponen, M. Kataja, and J. Timonen. “Permeability and effective porosity of porous media,” *Phys. Rev. E*., vol. 56, pp. 3319–3325, September 1997. DOI:10.1103/PhysRevE.56.3319.

[35] A. Duda, Z. Koza, and M. Matyka. “Hydraulic tortuosity in arbitrary porous media flow,” Phys. Rev. E., vol. 84, 036319 (pp. 1–8), September 2011. DOI:10.1103/PhysRevE.84.036319.

[36] K. Boomsma, and D. Poulikakos, “The effects of compression and pore size variations on the liquid flow characteristics in metal foams,” *J. Fluid Eng*., vol. 124, no. 1, pp. 263-272, 2001. DOI: 10.1115/1.1429637.

[37] A. Bhattacharya, V. V. Calmidi, and R. L. Mahajan, “Thermophysical properties of high porosity metal foams,” *Int. J. Heat Mass Tran*., vol. 45, no. 5, pp. 1017-1031, 2002. DOI: 10.1016/S0017-9310(01)00220-4.

[38] D. Cornell, and D. L. Katz, “Flow of gases through consolidated porous media,” I*nd. Eng. Chem*., vol. 45, no. 10, pp. 2145-2152, 1953. DOI: 10.1021/ie50526a021.

[39] J. M. Baloyo, “Open-cell porous metals for thermal management applications: fluid flow and heat transfer,” *Mater. Sci. Tech.*, vol. 33, pp. 265-276, May 2016. DOI: 10.1080/02670836.2016.1180795.

[40] E. Avalos-Gauna, and Y. Zhao, “Numerical simulation of heat transfer in porous metals for cooling applications,” *Metall. Mater. Trans. B*, vol. 48, no. 4, pp. 1925-1932, 2017. DOI: 10.1007/s11663-017-0981-1.

[41] D. J. Thewsey, and Y. Y. Zhao, “Thermal conductivity of porous copper manufactured by the lost carbonate sintering process,” *Phys. Status Solidi A*, vol. 205, no. 5, pp. 1126-1131, 2008. DOI: 10.1002/pssa.200723121.

[42] R. S. Vajjha, D. K. Das, and D. R. Ray, “Development of new correlations for the Nusselt number and the friction factor under turbulent flow of nanofluids in flat tubes,” *Int. J. Heat Mass Tran.*, vol. 80, pp. 353-367, January 2015. DOI: 10.1016/j.ijheatmasstransfer.2014.09.018.

[43] B. Bhushan, and R. Singh, “Nusselt number and friction factor correlations for solar air heater duct having artificially roughened absorber plate,” *Sol. Energy*, vol. 85, no. 5, pp. 1109-1118, 2011. DOI: 10.1016/j.solener.2011.03.007.

[44] F.W. Dittus, and L.M.K. Boelter, *Heat-Transfer in Automobile Radiators of the Tubular Type*. Publications in Engineering, Berkeley, USA, 1930.

[45] M. S. Bhatti, and R. K. Shah, “Turbulent and Transition Flow Convective Heat Transfer in Ducts,” in *Handbook of Single-Phase Convective Heat Transfer*, S. Kakac, R.K. Shah, and W. Aung, Eds. New York, USA: Wiley, 1987, pp. 4·1 – 4·84.

Table 1 Physical properties of copper and water

Property	**Value**
Thermal conductivity of copper, W/(m·K)	390
Density of water, kg/m^3	997
Viscosity of water, mPa·s	1.05
Thermal conductivity of water, W/(m·K)	0.61

List of Figures

Fig. 7: Relationship between form drag coefficient and permeability of LCS porous copper with different pore sizes.

Fig. 8: Variations in heat transfer coefficient with porosity for LCS porous copper (pore size: 425-710 μm) at different water flow rates.

Fig. 9: Heat transfer coefficients of LCS porous copper samples with a similar porosity (≈70%) and different pore sizes.

Fig. 10: Variations of Nusselt number and friction factor with porosity and Reynolds number (shown next to data points) for the samples with the same pore size of 425-710 μm.

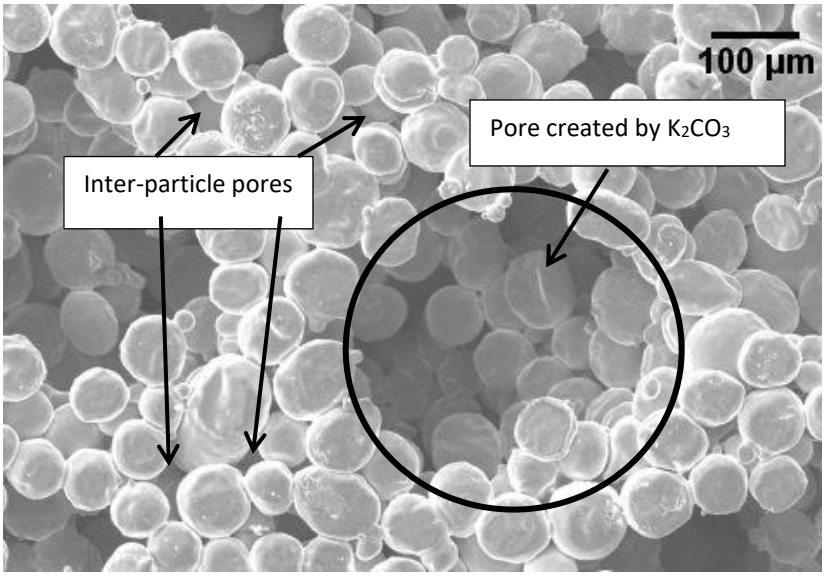

Fig. 2: SEM micrograph of LCS porous copper (68.6% porosity, 250-425 µm pore size) showing narrow inter-particle pores created through bonding of copper spheres, allowing connection of the large pores created by the K_2CO_3 particles.

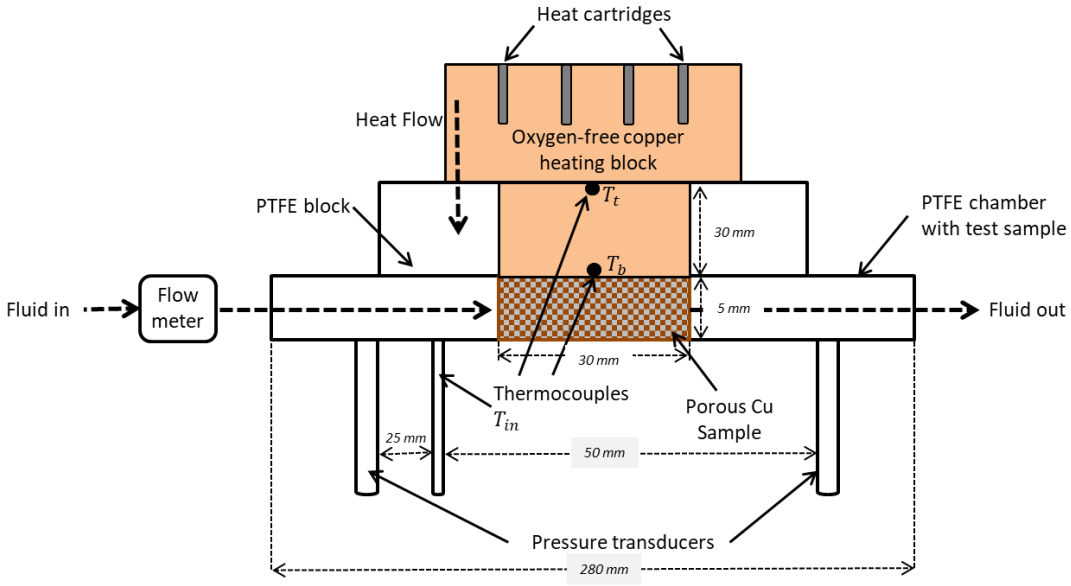

Fig. 2: Schematic diagram of the apparatus used for pressure drop and heat transfer coefficient measurements

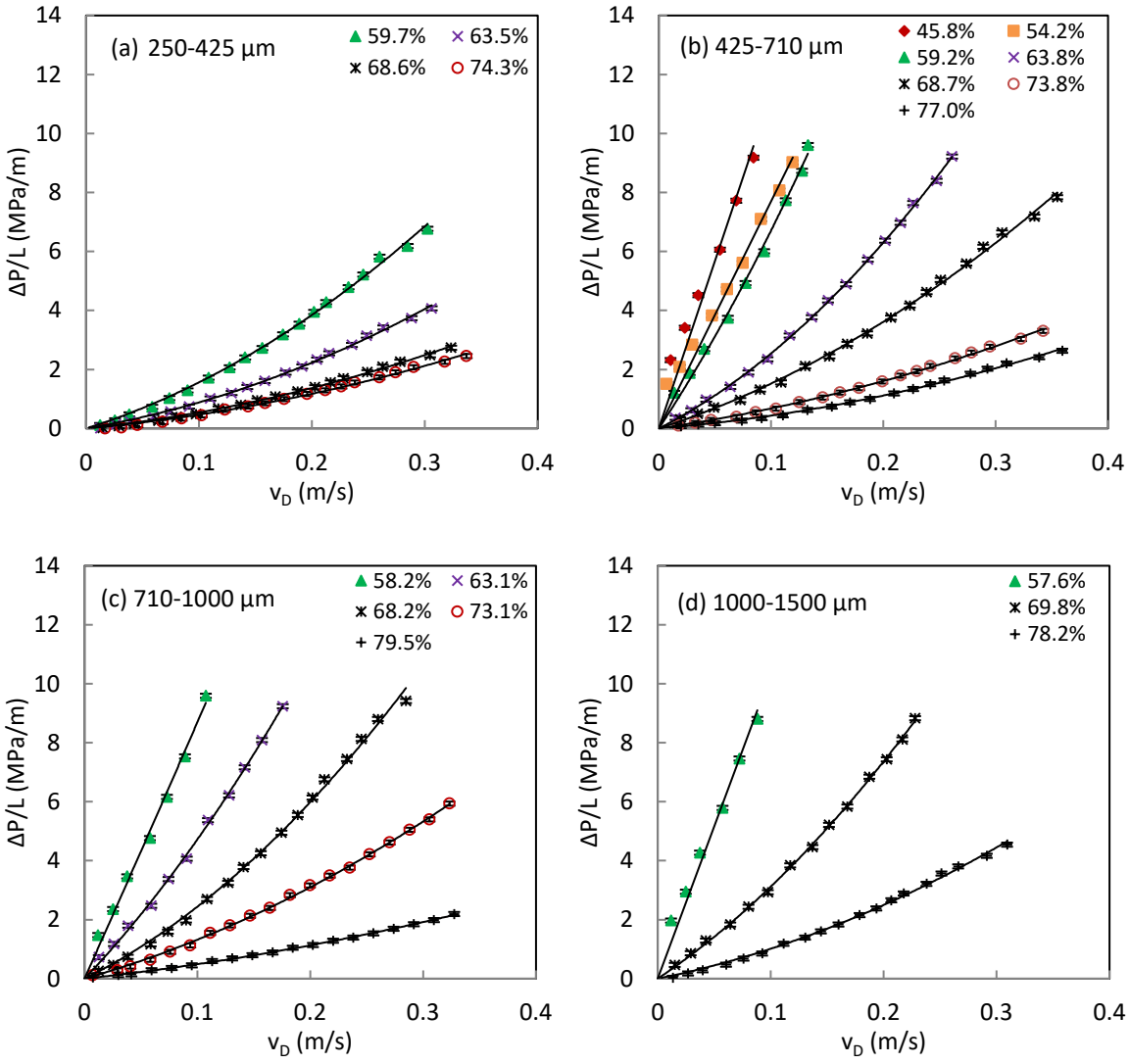

Fig. 3: Length-normalised pressure drop (ΔP/L) versus Darcian flow velocity (v_D) for LCS porous copper samples with different porosities (shown on graph) and pore sizes: a) 250-425 µm, b) 425-710 µm, c) 710-1000 µm and d) 1000-1500 µm.

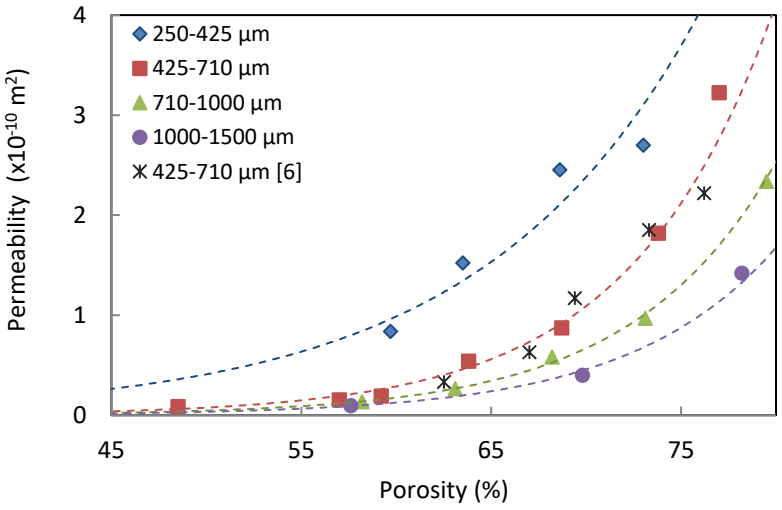

Fig. 4: Relationship between permeability and porosity of LCS porous copper with different pore sizes.

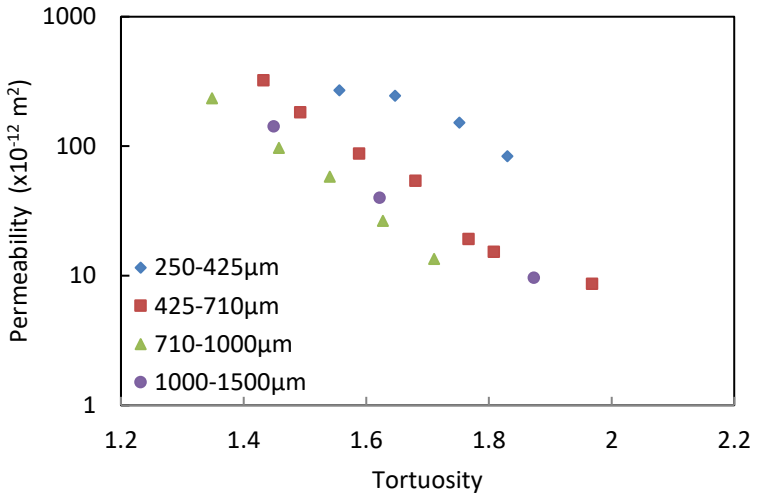

Fig. 5: Relationship between permeability and tortuosity of LCS porous copper with different pore sizes.

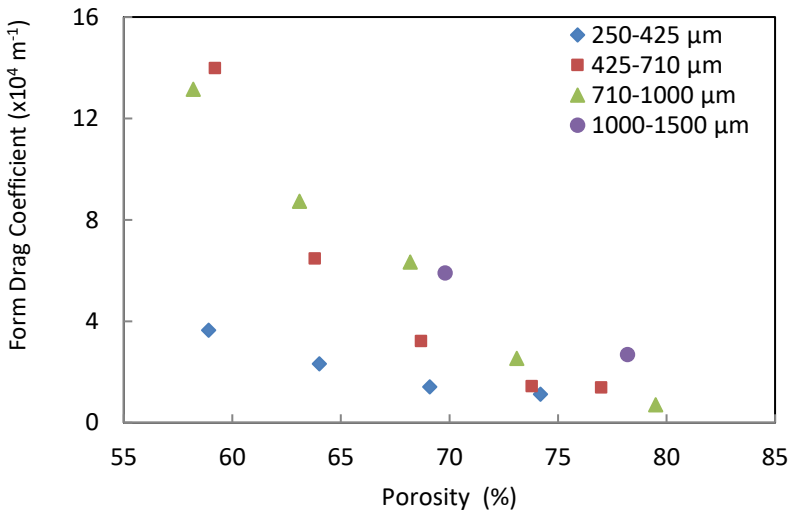

Fig. 6: Relationship between form drag coefficient and porosity of LCS porous copper with different pore sizes.

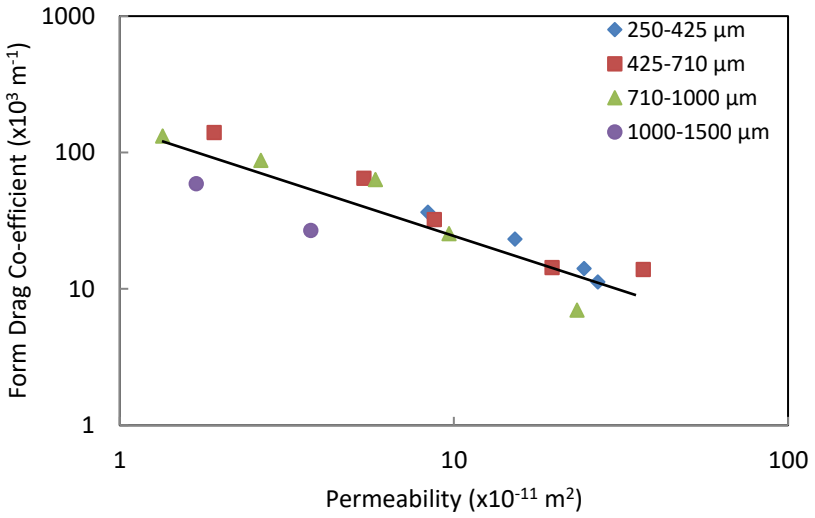

Fig. 7: Relationship between form drag coefficient and permeability of LCS porous copper with different pore sizes.

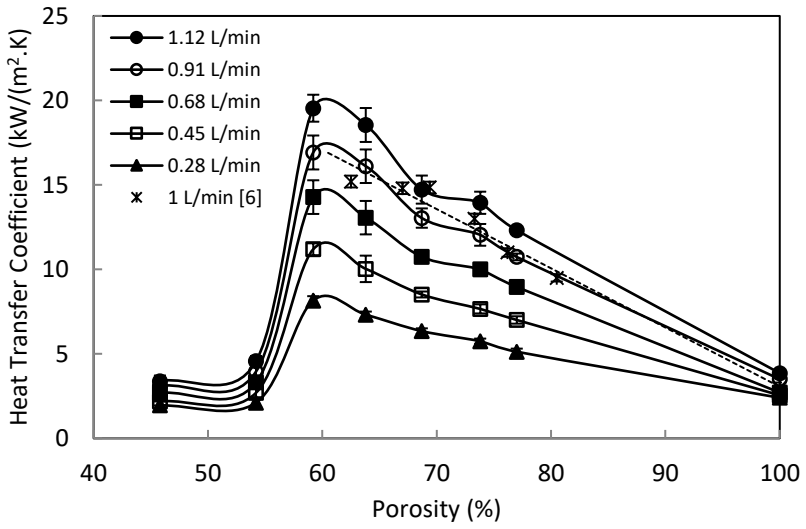

Fig. 8: Variations in heat transfer coefficient with porosity for LCS porous copper (pore size: 425-710 µm) at different water flow rates.

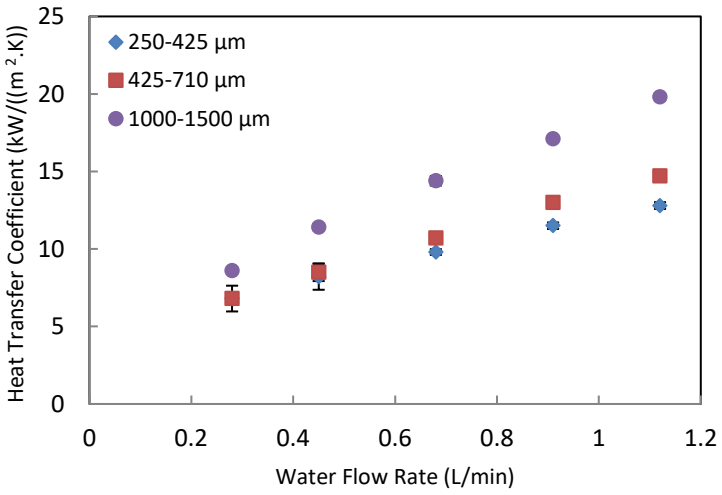

Fig. 9: Heat transfer coefficients of LCS porous copper samples with a similar porosity (≈70%) and different pore sizes.

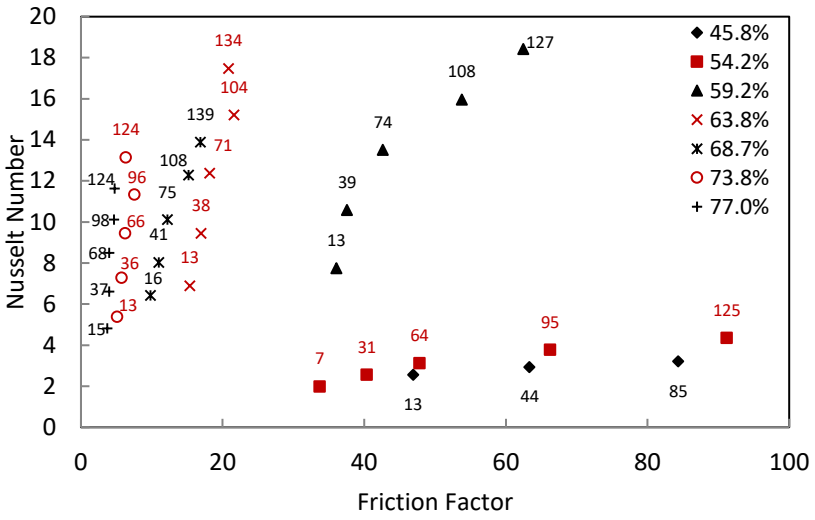

Fig. 10: Variations of Nusselt number and friction factor with porosity and Reynolds number (shown next to data points) for the samples with the same pore size of 425-710 µm.

Biographical note

Jan Mary Baloyo is an Honorary Research Associate in the University of Liverpool and Kings College London. She has a BSc(Hons) from the University of Nottingham, MSc and PhD from the University of Liverpool. Her research interests are in manufacture and characterisation of porous metals, and optimisation of porous metals for thermal management applications.

Yuyuan Zhao is a Professor in Materials Engineering in the University of Liverpool. He obtained his BEng and MSc degrees from Dalian University of Technology and a DPhil from Oxford University. He worked as a Lecturer at Dalian University of Technology and a Research Fellow at Birmingham University before he joined Liverpool University in 1998. His current research interests are in the manufacture, characterisation and application of porous materials. He was awarded the prestigious Ivor Jenkins Medal in 2015 by the Institute of Materials, Minerals and Mining for an outstanding contribution to powder metallurgy.